Low-frequency dielectric susceptibility of Li^+-doped KCl

C. Enss, M. Gaukler, S. Hunklinger, M. Tornow,* and R. Weis
Institut für Angewandte Physik der Universität Heidelberg, Albert-Ueberle-Strasse 3-5, D-69120 Heidelberg, Germany

A. Würger†
Institut für Theoretische Physik der Universität Heidelberg, Philosophenweg 19, 69120 Heidelberg, Germany
(Received 7 July 1995)

We report measurements of the complex dielectric susceptibility of lithium defects in potassium chloride (KCl:Li). Experiments were performed at a frequency of 10 kHz and at temperatures between 10 mK and 10 K on single crystals doped with either ^{6}Li or ^{7}Li. The lithium concentrations ranged from 4 ppm to 1100 ppm. At concentrations of a few ppm the lithium defects are well described as isolated tunneling systems. For the samples containing 60 ppm or more, we surprisingly observe that the dielectric susceptibility does not scale with the Li concentration. Moreover, we find a relaxation contribution, which indicates collective motion of the defects. Comparing our results with a recent theory based on a Mori approach, we find the motional spectrum of the defects to exhibit a crossover from coherent one-particle tunneling at concentrations below a few ppm to collective incoherent relaxation above 600 ppm. This dissipation mechanism is quite different from the usually considered relaxation based on the interaction with the phonon bath. Without any adjustable parameters, the theory accounts well for several measured quantities.

I. INTRODUCTION

Quantum tunneling in solids has been a subject of continuous research for over 30 years. Besides the tunneling excitations in various amorphous materials such as glasses and polymers, tunneling systems may arise from substitutional defects in crystals.[1,2] Lithium ions dissolved in KCl crystals (KCl:Li) form an example with a particularly simple structure, and are thus considered as a model for the tunneling of substitutional defects.

Early works gave a now generally accepted picture for a single, isolated defect in its symmetrical crystal environment. The considerably smaller lithium ion substitutes a potassium ion in the fcc lattice. Instead of occupying a centrosymmetrical lattice site, it prefers to dwell in one of eight equivalent positions in the $\langle 111 \rangle$ crystal directions.[3] A huge dipole moment is associated with the ion placed in one of these off-center positions, pointing towards a space diagonal and resulting in a strong coupling to external electric fields.

The properties of an isolated defect are well described by a theoretical model[4] that is based upon the tunneling motion between localized states. Quantum tunneling partially lifts the eightfold degeneracy of the ground state, leading to four equidistant energy levels with degeneracies 1-3-3-1. Recent paraelectric resonance experiments[5] showed excellent agreement with this model and allowed an accurate determination of its parameters.

Whereas the thermal properties of samples with very low lithium concentration could be explained by the tunneling of isolated defects (e.g., Ref. 6), serious discrepancies appeared at concentrations above about 100 ppm. In both the static dielectric constant of KCl:Li and in the complex dielectric response of various other defects in KCl additional features were reported.[7–10] Furthermore, measurements of the specific heat and the thermal expansion by Dobbs and Anderson[11] showed deviations from the expected Schottky anomaly. Besides a shift to higher energy, the experimental curve was considerably broadened and therefore related to a spectrum of excitations instead of the single energy splitting Δ_0.

Very early it was realized that the dipole-dipole interaction of adjacent defect ions was responsible for the observed anomalies. Klein[12] and Lawless[13] calculated independently the correlations between classical dipoles and pointed out how their interaction would lead to ''frozen'' dipole pairs, causing a reduction in the dielectric constant. Baur and Salzman[14] took quantum tunneling into account and performed a virial expansion. As an essential simplification they substituted the actual complicated eight-state system by a simpler two-state system. In a comprehensive study, Fiory[7] showed for various defect systems the existence of a threshold concentration, below which interaction was unimportant. Moreover, he observed very slow relaxation processes on the time scale of minutes. In a series of papers Klein refined the model of Baur and Salzman and calculated various static and dynamical quantities.[15,16] Kranjc solved the dynamical equation of a pair of two-level defects by considering the tunneling motion as a small perturbation.[17] Recently Terzidis obtained the exact dynamics and the statistical operator for such a pair.[18]

These works suffer from their truncation of the virial expansion after the first two terms. Because of this approximation, their results are valid only at low concentrations. However, very interesting phenomena occur at high concentrations, where the thermodynamic properties of the defects are significantly affected by the dipolar interaction, thus demanding a strong-coupling theory. A recent mode-coupling approach permits one to study the dynamical behavior of the defects in the whole range of concentrations.[19,20] The cases of both weak and strong coupling (i.e., low and high concentration) are treated on an equal footing. At low concentrations the mode-coupling

theory yields the same results as obtained previously from the virial expansion.

In the present paper we report measurements of the complex dielectric constant of KCl crystals doped with different Li isotopes. In order to study the influence of interactions between the Li ions on the dielectric properties, we have investigated samples with concentrations ranging from 4 ppm to 1100 ppm. The experimental results are discussed in the framework of the mode-coupling theory cited above. Preliminary results of this work have been published in Ref. 21.[22]

II. THEORY

Quantum tunneling in KCl:Li leads to quite different dynamical phenomena depending on the lithium concentration. Sufficiently diluted defects are well described as isolated tunneling centers with tunneling amplitude Δ_0, whereas with rising concentration c interactions between the lithium ions become more important.

In this section we first review the properties of an isolated defect and discuss the two-state approximation. Following this we present relevant theoretical models, which take the dipole-dipole interaction into account. Finally we summarize the main results of a recent approach based on Mori's reduction method.

A. Isolated tunneling defect

1. Energy spectrum

Tunneling defects in KCl:Li are formed by substituting a potassium ion in the fcc lattice of KCl with a Li^+. The difference between their ionic radii (1.33 Å for K^+ and 0.60 Å for Li^+), as well as their local polarization and repulsing ion core forces, is the reason why the centrosymmetrical (former K^+) position is not the energetically favored position for the substituent. Indeed, *ab initio* calculations[23] reveal off-center positions to be energetically more favorable and, moreover, agree with experimental results[3] indicating eight localized equivalent positions lying along the $\langle 111\rangle$ crystal symmetry directions,

$$\mathbf{r}=\frac{d}{2}(\alpha,\beta,\gamma), \tag{1}$$

with $\alpha,\beta,\gamma=\pm 1$. These eight positions form a cube of side length $d=$ 1.4 Å, as is schematically illustrated in Fig. 1. Because of its net charge, the lithium ion moving between these states carries a bare dipole moment $p=2.63$ D.[5]

Quantum tunneling between the off-center positions leads to a splitting of the ground state. According to Gomez *et al.*,[4] there are three different amplitudes for tunneling along the edges of the cube, along a face diagonal, and along a space diagonal. It turns out, however, that only the former is relevant. Denoting the states localized at the positions (1) by $|\alpha\beta\gamma\rangle$, this amplitude is given by the nondiagonal matrix element of the potential V of the lithium ion between any two adjacent states,

$$\eta\equiv\langle 1\,1\,1|V|1\,1-1\rangle. \tag{2}$$

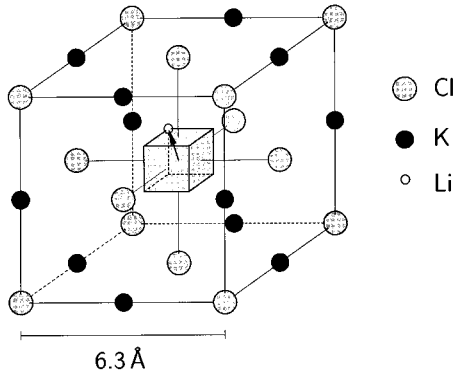

FIG. 1. The elementary fcc cell of KCl, the center K ion is replaced by an Li ion. Ion radii are reduced by a factor 1/5 for visibility. The arrow indicates the direction of the dipole moment.

The amplitudes along the face and space diagonals are negligible because of the higher barriers and the longer distance between the states involved.[4]

The energy eigenstates are irreducible representations of the point group O_h; they are constructed as superpositions of the localized states with appropriate phase factors,

$$|\mathbf{k}\rangle=8^{-1/2}\sum_{\alpha\beta\gamma}\exp\left(\frac{i\pi}{d}\mathbf{k}\cdot\mathbf{r}\right)|\alpha\beta\gamma\rangle, \tag{3}$$

where the entries of the vector $\mathbf{k}$ may take the values 0 and 1. The eight states are distributed among four equidistant levels,

$$\begin{aligned} E(A_{1g})&=-3\eta,\\ E(T_{1u})&=-\eta,\\ E(T_{2g})&=\eta,\\ E(A_{2u})&=3\eta, \end{aligned} \tag{4}$$

which are labeled according to their transformation behavior. The three-dimensional representations correspond to threefold-degenerate energies, which in terms of the vector $\mathbf{k}=(k_x,k_y,k_z)$ read

$$\begin{aligned} A_{1g}:&\quad (0,0,0);\\ T_{1u}:&\quad (1,0,0),\ (0,1,0),\ (0,0,1);\\ T_{2g}:&\quad (1,1,0),\ (1,0,1),\ (0,1,1);\\ A_{2u}:&\quad (1,1,1). \end{aligned} \tag{5}$$

The ground state (0,0,0) is totally symmetric and nondegenerate, as expected.

2. Selection rules for dipole transitions

Spectroscopy essentially relies on a linear coupling of the tunneling defect to a time-dependent elastic or electromagnetic field,

$$W=\mathbf{F}(t)\cdot\mathbf{r}, \tag{6}$$

where $\mathbf{r}$ is the defect's position operator (1) and $\mathbf{F}(t)$ is a periodic function of time. With (3) one easily derives that the

perturbation potential W induces only transitions between eigenstates whose $\mathbf{k}$ vectors differ by unity with respect to their absolute values:

$$|\langle \mathbf{k}|\mathbf{r}|\mathbf{k}'\rangle| = \frac{1}{2}d \quad \text{for } |\mathbf{k}-\mathbf{k}'|=1. \tag{7}$$

This selection rule results in a simple behavior for the position-position correlation function

$$\langle \mathbf{r}(t)\mathbf{r}\rangle = \frac{1}{4}d^2\cos(2\eta t), \tag{8}$$

where the angular brackets denote the thermal average $\langle\cdots\rangle \equiv \mathrm{tr}\cdots\exp(-H/k_BT)/\mathrm{tr}\,\exp(-H/k_BT)$.

3. Two-level approximation

For incident waves of sufficiently low amplitude, the potential (6) may be treated in lowest Born approximation or linear response theory. In this regime the lithium ion moving between its eight off-center positions cannot be distinguished from a two-level tunneling system with energy splitting 2η. Thus one is led to replace this complicated eight-state system by a simpler two-state system, which is most easily described using Pauli matrices $\sigma_x \equiv |L\rangle\langle R| + |R\rangle\langle L|$ and $\sigma_z \equiv |L\rangle\langle L| - |R\rangle\langle R|$, where $|L\rangle$ and $|R\rangle$ are localized states in a double-well potential, and $\sigma_z = \pm 1$ accounts for the defect dwelling in the left and right wells, respectively.[14]

Replacing the energy splitting by an effective tunneling amplitude $\Delta_0 = 2\eta$, the Hamiltonian for an isolated defect is given by

$$H = \frac{1}{2}\Delta_0\sigma_x. \tag{9}$$

The essential dynamical information is contained in the symmetrized two-time correlation function

$$G(t-t') = \frac{1}{2}\langle \sigma_z(t)\sigma_z(t') + \sigma_z(t')\sigma_z(t)\rangle, \tag{10}$$

whose spectrum can be calculated most easily with (9) by Fourier transformation,

$$G''(\omega) = \frac{\pi}{2}\sum_{\pm}\delta(\omega \pm \Delta_0/\hbar). \tag{11}$$

B. Dipole-dipole interaction

An ion with charge q moving between two localized states at $\mathbf{r} = \frac{1}{2}\mathbf{d}\sigma_z$ carries a dipole moment

$$\mathbf{p} \equiv q\mathbf{r} = \frac{1}{2}q\mathbf{d}\sigma_z, \tag{12}$$

thus giving rise to a dipolar interaction between neighboring defects i,j at a distance $\mathbf{r}_{ij} \equiv \mathbf{R}_i - \mathbf{R}_j$,

$$\frac{1}{4\pi\varepsilon\varepsilon_0}\frac{\mathbf{p}_i\cdot\mathbf{p}_j r_{ij}^2 - 3(\mathbf{p}_i\cdot\mathbf{r}_{ij})(\mathbf{p}_j\cdot\mathbf{r}_{ij})}{r_{ij}^5} \equiv \frac{1}{2}J_{ij}\sigma_z^i\sigma_z^j. \tag{13}$$

Accordingly the interacting tunneling defects are described by the Hamiltonian

$$H = \sum_i \frac{1}{2}\Delta_0\sigma_x^i + \sum_{\langle i,j\rangle}\frac{1}{2}J_{ij}\sigma_z^i\sigma_z^j, \tag{14}$$

where the sum in the coupling term runs over all pairs.

The random configuration of the defects on the host lattice leads to a distribution in the coupling energy J_{ij}, depending on both the distance r_{ij} and the relative orientation of the vectors $\mathbf{d}_i$, $\mathbf{d}_j$, and $\mathbf{r}_{ij}$. In order to simplify the distribution function for J_{ij}, we suppress the dependence on the relative orientation of $\mathbf{d}_i$, $\mathbf{d}_j$, and $\mathbf{r}_{ij}$, and write

$$\frac{1}{2}J_{ij} = \pm\frac{1}{4\pi\varepsilon\varepsilon_0}\frac{p^2}{r_{ij}^3} \tag{15}$$

instead of (13). Assuming in first approximation a continuous distribution in the distance r_{ij}, the distribution function of the interaction energy reads

$$P(J_{ij}) = \frac{1}{2}\frac{J_1J_2}{J_2-J_1}\frac{1}{J_{ij}^2} \tag{16}$$

for $J_1 \leqslant |J_{ij}| \leqslant J_2$. For N_0 lattic sites one obtains $J_1 = J_2/N_0$.[15,19] The upper cutoff J_2 is fixed by the condition $\int dJ_{ij}P(J_{ij}) = 1$. One finds

$$\frac{1}{2}J_2 = \frac{1}{4\pi\varepsilon\varepsilon_0}\frac{p^2}{a^3}, \tag{17}$$

with a being determined through the volume $(4\pi/3)a^3 = V/N_0 = c/n$. [Cf. the Appendix of Ref. 19. The definitions (15) and (17) differ from the notation used there by a factor of 2.] Here n denotes the number density (i.e., the number of defects per volume) and p the absolute value of the bare dipole moment (12).

For very close neighbors the continuum approximation (16) is not well justified since the possible spacings between lattice sites lead to discrete values of the coupling energy J_{ij}. Note that for KCl:Li the cutoff value J_2 is somewhat larger than that of nearest neighbor sites, $J_2 \approx 6.3J_{\mathrm{NN}}$. Both are by several orders of magnitude larger than the tunneling amplitude Δ_0.[19]

C. Dynamics

1. Pair model

At sufficiently low concentration, most lithium defects may be considered as isolated tunneling systems. The few remaining ones are involved in pairs; larger clusters comprising three or more defect ions occur with negligible probability. This assumption is an essential feature of most theoretical works on interacting tunneling defects.[14–18]

Considering a single pair of two-level systems with coupling energy $|J_{12}| \equiv J$ one finds as the relevant level spacings[14,15]

$$\eta_\pm \equiv \sqrt{\Delta_0^2 + \frac{1}{4}J^2} \pm \frac{1}{2}J; \tag{18}$$

accordingly the correlation spectrum exhibits four resonances,[18]

$$G''(\omega)=\frac{\pi}{2}\sum_{\pm}\frac{\eta_{\mp}}{\eta_+ + \eta_-}[\delta(\omega-\eta_{\pm}/\hbar)+\delta(\omega+\eta_{\pm}/\hbar)]. \tag{19}$$

For most pairs we have $J \ll \Delta_0$ and hence the resulting resonances differ little from the bare splitting ($\eta_{\pm}\approx\Delta_0\pm\frac{1}{2}J$) and (19) is equivalent to the spectrum of a single defect, Eq. (11). A small fraction of the defects interacts strongly ($\Delta_0 \ll J$), leading to $\eta_-\approx\Delta_0^2/J$ and $\eta_+\approx J$. Note in particular the presence of low-energy excitations $\eta_- \ll \Delta_0$. Strongly coupled pairs of tunneling states with very small energy splittings have been observed recently in various experiments.[24–26]

2. Mori theory

With rising concentration the defects can no longer be considered as isolated pairs, and interaction to more than a single neighbor has to be taken into account, indicating the break down of the pair model. As the most striking feature of such a many-body problem with disorder, correlation and response functions exhibit an important quasielastic or relaxational contribution. The spectral weight of the finite-energy excitations decreases accordingly.

In the framework of Mori's reduction method with a mode-coupling approximation, the motional spectrum arising from Hamiltonian (14) has been shown to exhibit both resonant and relaxational features. By applying a decoupling scheme on a continued fraction representation and solving the resulting integral equations self-consistently, an analytical expression for the spectral function has been derived.[19,20]

According to this approach, the dynamics changes significantly with rising concentration or number density n. This dependence is best discussed in terms of the dimensionless coupling parameter[27]

$$\mu\equiv\frac{cJ_2}{\Delta_0}\equiv\frac{2}{3}\frac{np^2}{\varepsilon\varepsilon_0\Delta_0}, \tag{20}$$

which measures the average interaction energy $np^2/4\pi\varepsilon\varepsilon_0$ in terms of the tunneling amplitude Δ_0. For very low concentration or $\mu \ll 1$, the mode-coupling theory yields a spectrum which is essentially identical to that of the pair model, Eq. (19).[20] With rising concentration, the correlation spectrum develops an additional pole at zero frequency and displays an effective three-pole structure,[28]

$$G_i''(\omega)=R_i\frac{\gamma_i}{\omega^2+\gamma_i^2}+\frac{1}{2}\sum_{\pm}(1-R_i)\frac{\Gamma_i}{(\omega\pm E_i/\hbar)^2+\Gamma_i^2}. \tag{21}$$

Thus the spectrum $G_i''(\omega)$ is comprised of a pair of complex poles at $i\Gamma_i\pm E_i/\hbar$ and a relaxation pole $i\gamma_i$. Both the poles and the residues depend on concentration or, equivalently, on the dimensionless parameter μ. For small μ the defect motion is dominated by weakly damped oscillations and accordingly the relaxation amplitude is small, $R_i \ll 1$. With rising concentration relaxation becomes more important. At $\mu\approx 1$ the amplitudes R_i strongly increase for most systems. For $\mu > 1$ one finds with $1-R_i \ll 1$ the motional spectrum to be dominated by relaxation.

The amplitudes R_i do not vary uniformly with μ and the spectrum $G_i''(\omega)$ depends on the defect site through the interaction energy

$$I_i^2\equiv\sum_j J_{ij}^2. \tag{22}$$

Calculation of observable quantities requires an appropriate average with respect to I_i and the corresponding distribution function reads $Q(I)=cJ_2I^{-2}\exp[c(1-J_2/I)]$.

The coupled density of states

$$D(E)=\sum_i (1-R_i)\,\delta(E-E_i) \tag{23}$$

is displayed in Fig. 1 of Ref. 20 for $\mu=1,2,3$. There are two well-separated features at energies above 1 K and well below 100 mK. The first one arises from single defects interacting with several neighbors at some average distance. Accordingly the energy splitting is shifted from the bare value Δ_0 towards higher energies with an average value of about $\Delta_0\sqrt{1+\mu^2}$. The low-energy peak is due to collective tunneling of pairs of nearby defects with tunneling amplitude Δ_0^2/I_i. In the limit of very low concentration, the density of states (23) reduces to a sharp peak at the bare tunneling splitting, $D(E)=\delta(E-\Delta_0)$ for $n\to 0$.

D. Susceptibility

For a weak external field all relevant dynamical information on the system is contained in the averaged linear response function

$$\chi(t-t')=\frac{1}{3V}\sum_i\frac{\mathrm{i}}{\hbar}\langle[\mathbf{p}_i(t),\mathbf{p}_i(t')]\rangle\Theta(t-t'); \tag{24}$$

the sum runs over all defects present in the sample of volume V. [For a discussion of correlations $\langle\mathbf{p}_i(t)\mathbf{p}_j(t')\rangle$, see Ref. 18.]

Fourier transformation gives the dynamical susceptibility $\chi(\omega)$ whose spectrum is connected to (16) through the fluctuation dissipation theorem

$$\chi''(\omega)=\frac{2}{3}np^2\tanh(\hbar\omega/2k_BT)\frac{1}{\hbar}\overline{G_i''(\omega)}, \tag{25}$$

where the overbar indicates the average over all defects, $\overline{\cdots}\equiv(1/N)\Sigma_i(\cdots)$, and where we have used the number density $n=N/V$. Thus the frequency dependence of $\chi''(\omega)$ is essentially determined by the spectrum (21).

The two parts of (21) result in quite different features in the dynamical response function. The first term gives rise to a relaxational contribution whose real and imaginary parts display characteristic relaxation peaks as functions of temperature. In the relevant frequency range, the second term contributes mainly to the real (or reactive) part of the susceptibility. For historical reasons, it is usually called the resonant contribution.

We thus write

$$\chi(\omega)=\chi_{\mathrm{res}}(\omega)+\chi_{\mathrm{rel}}(\omega), \tag{26}$$

where the real and imaginary parts of $\chi(\omega)\equiv\chi'(\omega)+i\chi''(\omega)$ are connected by the Kramers-Kronig relation.

The resonant part is determined by the well-known quantities $(1-R_i)$ and E_i,[20] and thus permits a thorough comparison with experiment. The relaxational contribution strongly depends on the rates γ_i, and since these are complicated function of the dipolar couplings J_{ij}, the theory is confined to qualitative statements with respect to relaxation.

At very low defect concentration the dipolar interaction is negligible, and the susceptibility is simply that of isolated two-level defects. For further use we note that in this case the static susceptibility is given by

$$\chi_{\rm iso}(\omega=0)=\frac{2}{3}\frac{np^2}{\varepsilon_0\Delta_0}\tanh\left(\frac{\Delta_0}{2k_BT}\right). \tag{27}$$

1. Resonant susceptibility

At low frequencies $\omega\ll E_i$, we may evaluate the resonant part of (26) at zero frequency. Moreover, using $\Gamma_i\ll E_i$ we find

$$\chi_{\rm res}(\omega=0)=\frac{2p^2}{3\varepsilon_0 V}\sum_i\ (1-R_i)\frac{1}{E_i}\tanh\left(\frac{E_i}{2k_BT}\right). \tag{28}$$

(The imaginary part vanishes for $\omega<\Delta_0^2/J_2$.)

The main peak in the density of states $D(E)$ results in a plateau for the resonant susceptibility. The low-energy excitations with $E_i\ll\Delta_0$, however, are relevant only at very low temperatures, but their spectral weight is small compared to that of the main peak above 1 K. For this reason we have discarded the low-energy exciations when calculating the plateau value $\chi_{\rm res}(0)$ at $T=0$.

The solid line in Fig. 8, below, is derived from a simplified analysis using the following approximate expressions: the distribution function $\tilde{Q}(I)=cJ_2/I^2$ for $cJ_2\ll I\ll J_2$, the energy $E_i=\sqrt{\Delta_0^2+I_i^2}$, and the residue $(1-R_i)=\Delta_0^2/E_i^2$ (for a discussion, cf. Refs. 19 and 20). We thus obtain

$$\chi_{\rm res}=\frac{2}{3}\frac{np^2}{\varepsilon_0}\int_{cJ_2}^{J_2}dI\,\frac{cJ_2\Delta_0^2}{I^2(\Delta_0^2+I^2)^{3/2}}\tanh\left(\frac{\sqrt{\Delta_0^2+I^2}}{2k_BT}\right). \tag{29}$$

After approximating the temperature-dependent factor by $\tanh(\Delta_0\sqrt{1+\mu^2}/2k_BT)$, which does not depend on I, integration yields in a straightforward fashion

$$\chi_{\rm res}=\frac{2}{3}\frac{np^2}{\varepsilon_0\Delta_0}\frac{(\sqrt{1+\mu^2}-\mu)^2}{\sqrt{1+\mu^2}}\tanh\left(\frac{\Delta_0\sqrt{1+\mu^2}}{2k_BT}\right). \tag{30}$$

In the limit of low concentration $\mu\to 0$, Eq. (30) reduces to the result for isolated defects, Eq. (27).

At zero temperature the relaxational contribution $\chi_{\rm rel}$ vanishes; using (27) we find the ratio

$$\frac{\chi}{\chi_{\rm iso}}=\frac{(\sqrt{1+\mu^2}-\mu)^2}{\sqrt{1+\mu^2}}\quad\text{at}\quad T=0, \tag{31}$$

which accounts for the concentration dependence of the zero-temperature static susceptibility. In the limit of low concentration ($c\ll J_2/\Delta_0$ or $\mu\ll 1$), Eq. (31) is equal to unity, whereas in the opposite limit it decreases with μ^{-3}. Thus the resonant susceptibility per defect diminishes for $\mu\gg 1$. Accordingly the average relaxation amplitude increases from zero to unity in going from $\mu\ll 1$ to $\mu\gg 1$.

2. Relaxational susceptibility

Now we turn to the relaxation contribution which arises from the quasielastic part of the correlation spectrum (21). The second term in (26) depends strongly on the relaxation rate $1/\tau_i=\gamma_i$, contrary to the resonant part, where the width Γ_i could be neglected in the frequency range of interest. Because of the random defect configuration, the rate γ_i shows a broad distribution; as a consequence the average of the relaxation susceptibility turns out much more complicated than that of the resonant part.

Here we resort to an approximate treatment which permits an explicit evaluation of $\chi_{\rm rel}(\omega)$. First we use a simplified expression for the relaxation rate derived in Ref. 20,

$$\gamma_i=\pi f D(E_i)[\cosh(E_i/2k_BT)]^{-2}\equiv f\xi_i, \tag{32}$$

with $fD(E_i)=\Sigma_j J_{ij}^2\delta(E_i-E_j)$. The quantity f is distributed according to $P_f(f)=\ln(f_{\rm max}/f_{\rm min})^{-1}f^{-1}\equiv K/f$ where the upper cutoff is given by $f_{\rm max}=cJ_2^2$ and the lower $f_{\rm min}$ is smaller by many orders of magnitude.[20] The last factor in (32) leads to an Arrhenius type of temperature dependence for $T<E_i$. As a second approximation we replace the energies E_i by the mean value $E=\Delta_0\sqrt{1+\mu^2}$.

We start with the real part of the relaxational susceptibility. Using $\hbar\omega/k_BT\ll 1$ and summing over all defects we obtain

$$\chi'_{\rm rel}(\omega)=\frac{p^2}{3\varepsilon_0 V}\frac{1}{k_BT}\sum_i\ R_i\frac{\gamma_i^2}{\omega^2+\gamma_i^2}. \tag{33}$$

Inserting (32) and averaging with respect to f we find

$$\sum_i\ R_i\frac{\gamma_i^2}{\omega^2+\gamma_i^2}=\sum_i\ R_i\int df P_f(f)\frac{f^2}{f^2+\omega^2/\xi^2}$$
$$=\sum_i\ R_i\frac{1}{2}K\ln\frac{\omega^2+f_{\rm max}^2\xi_i^2}{\omega^2+f_{\rm min}^2\xi_i^2}. \tag{34}$$

Simplifying further we replace the energies E_i by E and put $\xi=\pi D(E)\cosh(E/2k_BT)^{-2}$,

$$\chi'_{\rm rel}(\omega)=\frac{1}{3}\frac{np^2}{\varepsilon_0}r_0K\frac{1}{k_BT}\ln\frac{\omega^2+f_{\rm max}^2\xi^2}{\omega^2+f_{\rm min}^2\xi^2}, \tag{35}$$

where $r_0\equiv(1/N)\Sigma_i R_i$ denotes the averaged relaxation amplitude. From (35) we obtain the correct high-temperature limit $\chi'=\frac{1}{3}np^2r_0/\varepsilon_0k_BT$ for $T\gg T^*$, as expected from more general considerations. Thus $\chi'_{\rm rel}(\omega)$ increases from zero at $T=0$, goes through a maximum at T^*, and falls off as $1/T$ at high temperature.

Now we turn to the dissipative part

$$\chi''_{\rm rel}(\omega)=\frac{p^2}{3\varepsilon_0 V}\frac{1}{k_BT}\sum_i\ R_i\frac{\omega\gamma_i}{\omega^2+\gamma_i^2}, \tag{36}$$

whose main contribution stems from systems with $\omega\approx\gamma_i$. Proceeding as above, we find

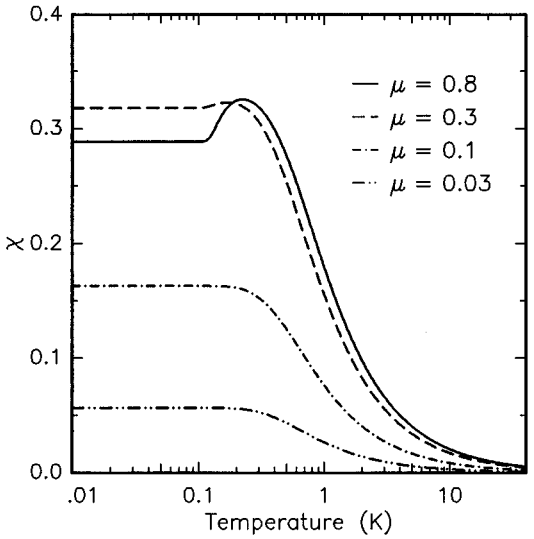

FIG. 2. Real part of the dielectric susceptibility calculated according to Eqs. (30) and (35).

$$\chi''_{\rm rel}(\omega)=\frac{p^2}{3\varepsilon_0 V}\frac{K}{k_B T}\sum_i R_i\left(\arctan\frac{f_{\max}\xi_i}{\omega}-\arctan\frac{f_{\min}\xi_i}{\omega}\right). \tag{37}$$

The second term is negligible for $f_{\min}\xi/\omega \ll 1$. For a single energy $E\equiv\Delta_0\sqrt{1+\mu^2}$, Eq. (37) becomes

$$\chi''_{\rm rel}(\omega)=\frac{1}{3\varepsilon_0}np^2 r_0 K\frac{1}{k_B T}\arctan\frac{f_{\max}\xi}{\omega}. \tag{38}$$

As the real part, $\chi''_{\rm rel}$ exhibits a maximum, with the crossover temperature being determined by $f_{\max}\xi=\omega$,

$$k_B T^*=\frac{\Delta_0\sqrt{1+\mu^2}}{\ln[\pi f_{\max}D(E)/4\omega]}. \tag{39}$$

The logarithmic variation with frequency is a general and well-known feature of a thermally activated relaxation process; in the present case the activation energy is provided by $\Delta_0\sqrt{1+\mu^2}$, restricting validity of the law (39) to temperatures well below 1 K.

At very low temperature the Arrhenius behavior of (32) leads to a sharp decrease of $\chi_{\rm rel}$. In the opposite limit all rates fulfill $\omega<\gamma_i$; then the factor $(1/T)$ results in a decrease with inverse temperature. (At still higher temperature fulfilling $f_{\min}\xi\gg\omega$, the dissipative part decreases even more rapidly.) According to Eqs. (33) and (36) both real and imaginary parts exhibit a relaxation maximum.

The classical high-temperature susceptibility for dipole relaxation is given by $np^2/3\varepsilon_0 k_B T$, whereas Eqs. (33) and (38) involve additional factors r_0 and K. Proceeding as above the averaged relaxation amplitude $r_0=(1/N)\Sigma_i R_i$ reads

$$r_0=\mu\left(\frac{\pi}{2}-\arctan(\mu)\right). \tag{40}$$

Accordingly r_0 vanishes in the limit of zero concentration or $r_0=\mu\pi/2$ for $\mu\ll 1$, and it reaches unity as $r_0=1-\mu^{-2}$ in the opposite case ($\mu\gg 1$). The second factor $K=\ln(f_{\max}/f_{\min})^{-1}$ arises from the distribution of the relaxation rate γ.

In order to illustrate the emergence of a relaxation peak, we show in Fig. 2 the real part of the susceptibility as a function of temperature, as given by Eqs. (30) and (35). The parameters are chosen in view of experimental data presented below; we have put $\omega=10$ kHz, $\pi f_{\max}D(E)=10^8$ Hz, and $K=10^{-3}$.

In the limit of zero temperature, the susceptibility is given by the resonant contribution (30), whereas the relaxational part results in maximum at about 100 mK. The relaxation peak is hardly visible for $\mu<\frac{1}{10}$; it gets more pronounced with rising concentration. We remark that the rate distribution discussed below Eq. (32) is probably too sharply peaked and thus results in too narrow a relaxation maximum. (Our neglecting the low-energy excitations leads to a sharp cutoff below about 100 mK.) Though it might modify some special features, a more detailed analysis is expected to leave invariant the general features shown in Fig. 2.

III. EXPERIMENTAL TECHNIQUE

All samples investigated in our measurements were KCl single crystals doped with different concentrations of Li as grown from the melt at the Crystal Growth Laboratory of the University of Utah in Salt Lake City. The starting materials had been pretreated to reduce the OH^- impurity concentration to typically less than 0.2 ppm.[29] The ^{7}Li introduced to the melt was a natural isotope mixture containing 7.4% ^{6}Li, while the ^{6}Li introduced to the melt was reported to be $>95\%$ ^{6}Li. The actual Li concentrations were determined by flame emission spectroscopy. The samples containing 60 ppm ^{7}Li and 70 ppm ^{6}Li have been investigated previously in specific heat and thermal expansion experiments[11] and were provided by A. C. Anderson, University of Illinois, for our dielectric measurements. All other samples were specially grown for the work discussed in this article.

To obtain flat disks about 2 mm thick and 15 mm in diameter, necessary for our dielectric experiments, we have cleaved the crystals along the $\langle 100\rangle$ direction. Since aging effects on KCl:Li crystals have been reported earlier,[3] we heated the samples briefly over 350 °C and quenched them to room temperature immediately before the experiments. Next the samples were mounted in a sample holder, attached to the mixing chamber of a dilution refrigerator, and the cool down was started. The crystals containing 4 ppm, 60 ppm, and 600 ppm Li have been measured both before and after quenching. We did not observe any difference caused by this treatment for the 60 ppm and 600 ppm samples, while the total variation of susceptibility of the 4 ppm sample was reduced by about 5% after quenching.

The dielectric susceptibility of the KCl:Li samples was measured using a noncommercial bridge circuit. It consists of an inductive voltage divider, a resistance decade, and a lock-in amplifier as null balancing detector. To improve the resolution of our measurement we have integrated the reference capacitor, a sapphire disk 3 mm thick and 20 mm in diameter with evaporated gold electrodes, into the sample holder. The high symmetry and stability of this design results in a very low level of pickup noise. At temperatures below

20 K the dielectric constant of sapphire is independent of temperature and its dielectric loss is negligible. This has been verified by a run without a sample. In balance the real part of the dielectric constant is determined by the setting of the voltage divider and the dielectric loss is compensated by the resistance decade. The temperature was measured using a carbon resistance thermometer attached to the sample holder and by the magnetic susceptibility of a cerium magnesium nitrate (CMN) thermometer located in the mixing chamber.

IV. RESULTS

A. Local field correction

Because of the permittivity of the KCl:Li crystal, the electric field experienced by the defect ions is not the same as the external field applied to the sample. In order to conclude from a macroscopic quantity such as the dielectric function on the microscopic behavior of a given tunneling system, the polarization of both the host crystal and the neighboring defects has to be taken into account. Indeed the quantum mechanical response function (24) is calculated with respect to the local field. When comparing the measured dielectric function with the dynamical susceptibility defined in Sec. II, the data are always plotted taking into account corrections for the local field.

A simple way to derive an approximate expression for the local field $F_{\rm loc}$ has been developed by Lorentz (see, for example, Ref. 30). For the limits of low and high defect concentration, different corrections have to be applied. At very low concentration the contribution of the tunneling ions to the local field can by neglected, because their dipole field vanishes at large distances. Therefore the correction is determined by the polarization of the host crystal. In this limit one obtains an expression for the dielectric susceptibility similar to the well-known Clausius-Mossotti equation, where only the dielectric constant of the vacuum is replaced by $\varepsilon_{\rm KCl}$:

$$\chi = \frac{3(\varepsilon - \varepsilon_{\rm KCl})}{\varepsilon_{\rm KCl} + 2}. \tag{41}$$

Here $\varepsilon_{\rm KCl}$ denotes the low-temperature value of the dielectric constant of a pure KCl crystal. From our measurements we obtain $\varepsilon_{\rm KCl} = 4.49$ at 4 K in agreement with values reported earlier.[31,32] This value has been used in the analysis of our data.

At high Li concentration the tunneling dipoles contribute significantly to the local field, and the susceptibility is given by

$$\chi = \frac{9(\varepsilon - \varepsilon_{\rm KCl})}{(\varepsilon + 2)(\varepsilon_{\rm KCl} + 2)}. \tag{42}$$

In the case of KCl:Li the numerical values of the susceptibility obtained using Eqs. (41) and (42) differ roughly by a factor of 2; i.e., at high concentrations one would expect that the difference $\varepsilon - \varepsilon_{\rm KCl}$ per defect is about twice as high as for low concentrations. The behavior for intermediate concentrations is difficult to calculate, and the range of validity of the limiting expressions is not well defined. For the analysis of our data we have assumed that for the samples containing 4 ppm and 6 ppm Eq. (41) is valid, since the total variation of ε was only in the order of 2%. For all other samples we have used Eq. (42) in order to account for the local field correction.

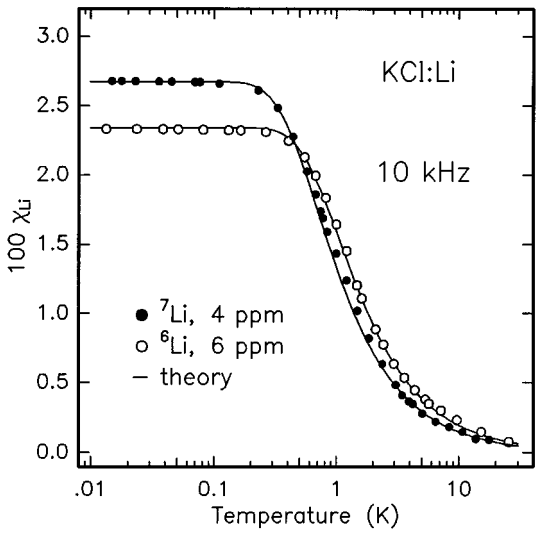

FIG. 3. Real part of the dielectric susceptibility of KCl crystals doped either with 4 ppm ^{7}Li and 6 ppm ^{6}Li at 10 kHz. Solid lines are theoretical curves using Eq. (30).

B. Temperature dependence

Figure 3 shows the temperature dependence of the real part of the dielectric susceptibility at 10 kHz of two KCl crystals doped with a few ppm of different Li isotopes (^{6}Li, ^{7}Li). As discussed in the previous section the data are plotted taking into account the local field correction, which allows a direct comparison with Eq. (30), which in fact is identical to Eq. (27) at such low concentrations. The solid lines are theoretical curves for the dielectric susceptibility of isolated Li tunneling systems calculated using the values $^7\Delta_0/k_{\rm B} = 1.1$ K, $^6\Delta_0/k_{\rm B} = 1.65$ K, and $p = 2.63$ D from Ref. 5.[33] The Li concentrations used in our fits agree with those determined by flame emission spectroscopy within the error limits of this technique. The very good agreement of the calculated curves and the data demonstrates the validity of the two-level description for isolated Li tunneling states.

As shown in Fig. 4 the susceptibility observed for the samples with 60 ppm ^{7}Li and 70 ppm ^{6}Li at a frequency of 10 kHz looks still very much like that of isolated defects. The temperature dependence is well described by a hyperbolic tangent. However, in both cases the prefactor is smaller than expected for isolated tunneling systems. This and the appearance of a tiny maximum around 200 mK are first signs that the interaction among the Li tunneling states become relevant.

The imaginary part $\chi''(\omega)$ provides additional evidence for the importance of the dipolar interaction. In the frequency range of our experiments the dielectric absorption arises exclusively from relaxational contributions. As discussed in Sec. II, one would not expect any relaxation absorption for isolated Li tunneling systems [cf. Eq. (27)]. Fig-

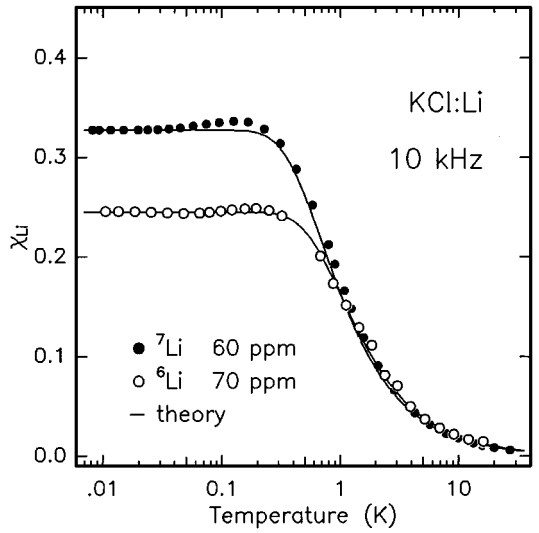

FIG. 4. Real part of the dielectric susceptibility of KCl crystals doped with different Li isotopes at 10 kHz. Solid lines are fits using Eq. (30).

ure 5 shows the temperature dependence of ε'' at 10 kHz for samples containing different isotopes. For both samples an absorption peak below 200 mK is observed, which clearly indicates the occurrence of relaxation. The magnitude of the absorption and the temperatures at which the peaks occur depend on the Li isotope. Surprisingly the absorption of the sample with lower lithium concentration is higher in the whole temperature range. Since relaxational absorption processes are most effective for systems fulfilling $\omega = \gamma_i$, this result indicates that the relaxation rate depends on the isotope mass in a complicated manner.

At still higher concentrations we find more pronounced relaxation contributions. The absorption maximum gets broader and extends to the lowest temperatures investigated, thus indicating the existence of systems with small excitation energies.

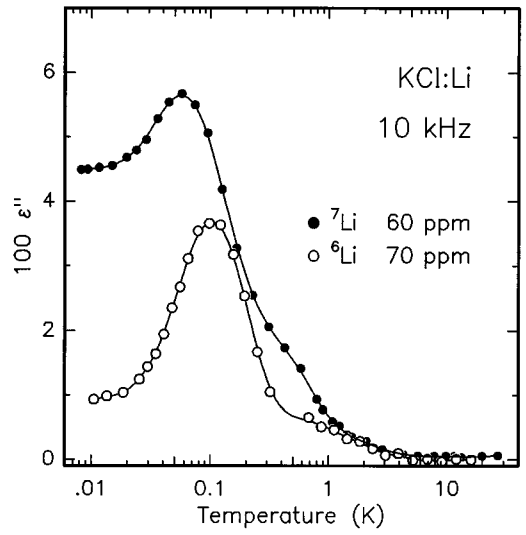

FIG. 5. Imaginary part of the dielectric constant of KCl crystals doped with different Li isotopes at 10 kHz. Solid lines are guides for the eyes.

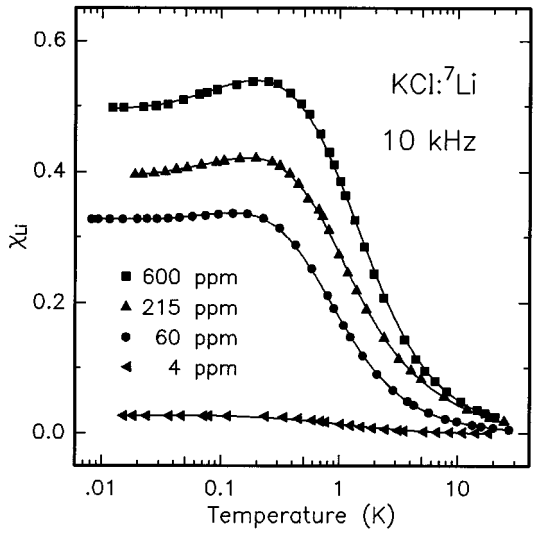

FIG. 6. Real part of the dielectric susceptibility of KCl crystals doped with four different ^{7}Li concentrations at 10 kHz. Solid lines are guides for the eyes.

C. Concentration dependence

According to the theory discussed in Sec. II, the concentration of the tunneling dipoles is an essential parameter. In Figs. 6 and 7 the dielectric susceptibility is displayed for four different concentrations of each isotope. Let us start with the ^{7}Li samples (Fig. 6). Although at a first glance all curves look similar, it is immediately evident that the susceptibility does not scale linearly with the Li concentration. This becomes most obvious by comparing the results for the 60 ppm and the 600 ppm samples, where the total variation of χ differs only by a factor of 1.5, whereas the ratio of the Li concentrations is 10. Clearly at concentrations above 100 ppm the properties of KCl:Li cannot be described as a dilute defect system. We observe very similar results for the ^{6}Li samples shown in Fig. 7. Here the low-temperature value of

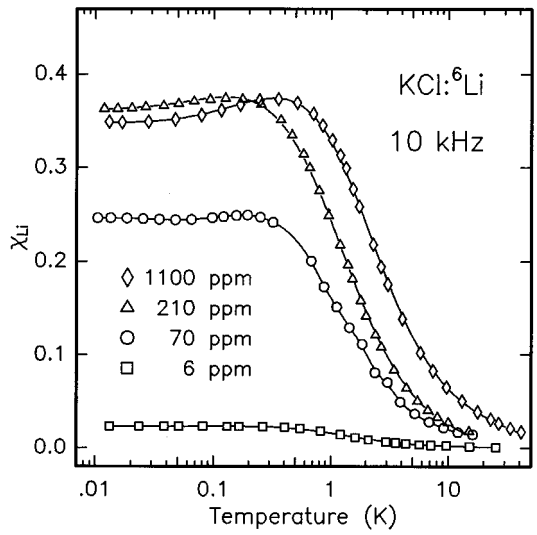

FIG. 7. Real part of the dielectric susceptibility of KCl crystals doped with four different ^{6}Li concentrations at 10 kHz. Solid lines are guides for the eyes.

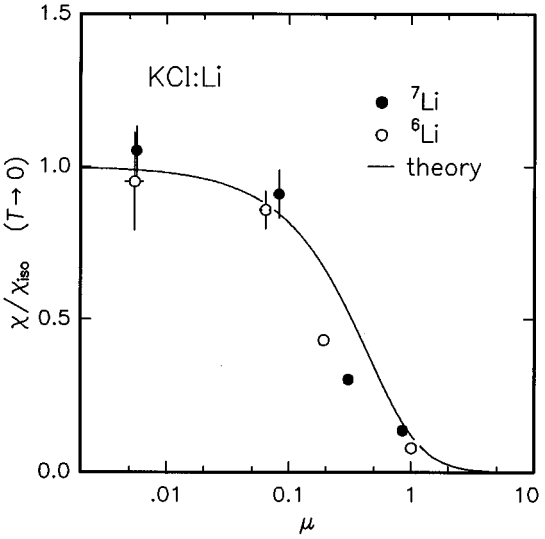

FIG. 8. Normalized low-temperature value of real part of the dielectric susceptibility of KCl:Li $\chi/\chi_{\rm iso}$ as a function of $\mu=(2np^2)/(3\varepsilon\varepsilon_0\Delta_0)$. The solid line is a theoretical curve calculated with Eq. (31).

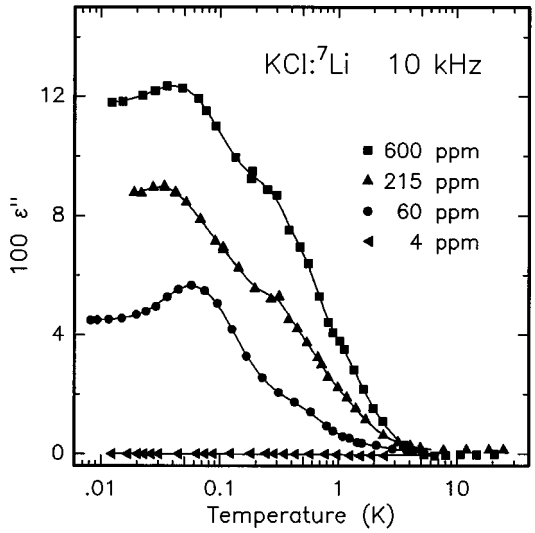

FIG. 9. Imaginary part of the dielectric constant of KCl doped with four different ^{7}Li concentrations at 10 kHz. Solid lines are guides for the eyes.

the susceptibility is even smaller for the 1100 ppm sample as compared to the crystal containing 210 ppm. In addition the expected shift of the $1/T$ dependence towards higher temperatures according to Eq. (30) is clearly visible in this case.

In Fig. 8 the normalized low-temperature value of the dielectric susceptibility $\chi/\chi_{\rm iso}$ of all samples is plotted as a function of the dimensionless parameter μ [cf. Eq. (20)]. The solid line in Fig. 8 represents the theoretical curve calculated using Eq. (31). Given the fact that no parameter is adjustable, theory and experiment agree remarkably well. From this we conclude that the Mori approach discussed in Sec. II allows a quantitative understanding of the defects in KCl:Li.

As a second unmistakable indication for the presence of an interaction among the tunneling states, we find an increasing relaxation contribution with rising Li concentration. In the temperature dependence of the real part of the susceptibility this leads to a maximum between 100 mK and 500 mK. Note that the peak becomes more pronounced with increasing concentration. Analogous observations have been made previously by Fiory[7] in measurements of the dielectric constant of KCl:Li and other defect systems at much lower frequencies of about 0.016 Hz. Since the temperature where the maximum occurs was found to be proportional to np^2, he concluded that the electrical dipole-dipole interaction among the tunneling states is responsible for its occurrence.

Our measurements of the imaginary part of the dielectric constant confirm that the maximum in the real part is due to relaxation processes. In Figs. 9 and 10 the results of such measurements are displayed for four different concentrations of each isotope. Within the error of our experiments we find no dielectric absorption for the samples with the lowest concentrations (4 ppm and 6 ppm) in the whole temperature range. This again proves that the Li tunneling states at such low concentration may be considered as isolated systems. For samples with higher defect concentrations we find an increasing relaxational absorption, which is most significant at temperatures well below 1 K. According to the theory of Sec. II this indicates a broad distribution of relaxation rates.

D. Time and frequency dependences

During the measurements on samples with high defect concentrations we noticed that at low temperatures it took as long as 3 h to reach a stationary value of ε after the temperature has being changed. An example of this unexpected behavior is shown in Fig. 11. Let us look for instance at the variation of the dielectric constant when the temperature of the sample is increased from 42 mK to 52 mK. Although the temperature has already reached a steady value after a few minutes, the dielectric constant is still varying well over an hour later. The fact that the system reaches thermal equilib-

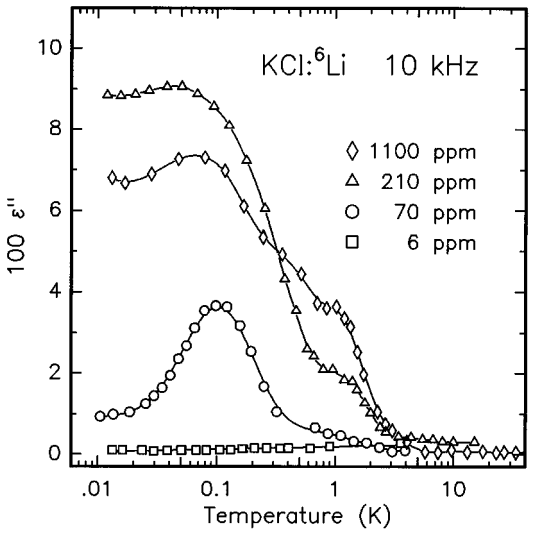

FIG. 10. Imaginary part of the dielectric constant of KCl doped with four different ^{6}Li concentrations at 10 kHz. Solid lines are guides for the eyes.

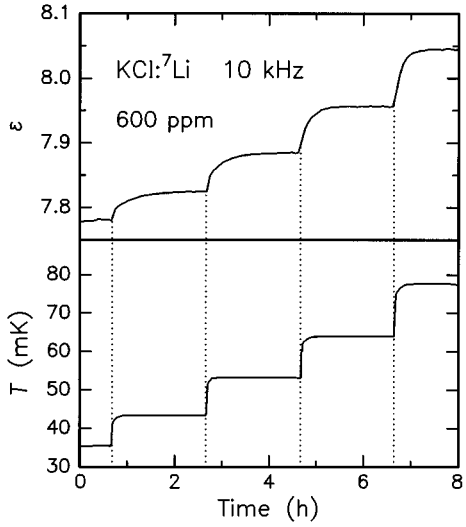

FIG. 11. Upper curve: time dependence of real part of the dielectric constant of a KCl crystal containing 600 ppm ^{7}Li while changing the temperature. Lower curve: temperature of the sample as a function of time.

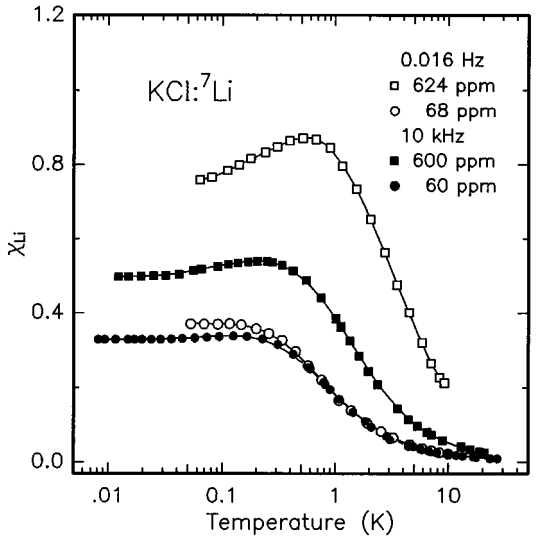

FIG. 12. Temperature dependence of the real part of the dielectric susceptibility of KCl:Li at different frequencies. The data at 0.016 Hz are from Ref. 7. Solid lines are guides for the eyes.

rium so slowly indicates that a considerable fraction of the tunneling states has extremely long relaxation times.

From the concentration dependence we may conclude that this behavior is an intrinsic property of the defect system and not due to any technical problems. For samples with 60 ppm a delay of the dielectric constant is hardly noticeable, but with increasing concentration the the time needed to reach the equilibrium value of the dielectric constant becomes longer and longer. At first glance one might be surprised that we see contributions of such slow relaxing systems at all, because our measuring frequency is 10 kHz, and we therefore observe mainly systems which fulfill the condition $\omega \leqslant \tau^{-1}$. However, since any changes of the polarization of the crystal will change the local field, the susceptibility of fast tunneling states will be modified by slowly relaxing neighboring states via the variation of the local field.

The fact that we observe dielectric absorption at 10 kHz and simultaneously tunneling states with relaxation times as long as an hour proves that at high Li concentrations a very broad distribution of relaxations times exists. This agrees well the nearly constant distribution of relaxation rates observed in frequency-dependent measurements of the dielectric function reported previously in Ref. 7. Such a wide distribution of relaxation times and especially the extension of the relaxation spectrum to very long time scales have been derived theoretically as discussed in Sec. II (cf. Ref. 20). Based on this theory we can interpret the relaxation mechanism as a collective motion involving many tunneling systems. Note that such a process is quite different from the usually considered one-phonon process.[34]

To demonstrate the frequency dependence of the dielectric susceptibility at different Li concentrations we have plotted Fiory's data[7] together with our results in Fig. 12. Although the measuring frequencies differ by more than five orders of magnitude, we find hardly any frequency dependence for the 60 ppm and the 68 ppm samples. The somewhat higher total variation of χ for the 68 ppm sample reflects simply the difference in lithium concentration. In contrast, we find a strong frequency dependence for the high-concentrated samples, indicating that collective relaxation processes dominate the dielectric susceptibility of these samples.

V. DISCUSSION

A. Collective dynamics

The theory sketched in Sec. II provides a crossover from one-particle tunneling at low concentrations to collective dynamics for sufficiently high defect density, occurring at $\mu = 1$. (This condition is met at concentrations of $c \simeq 600$ ppm for ^{7}Li and at $c \simeq 1050$ ppm for ^{6}Li.)

Several novel features in the motional spectrum have been shown to arise from the dipolar coupling to adjacent ions.[20] First, the one-particle excitations are shifted from the bare tunneling splitting Δ_0 to higher values at about $\Delta_0\sqrt{1+\mu^2}$ [cf. Eq. (30)]. Second, for a small number of nearby pairs of defects, the strong coupling leads to tunneling motion with a energy splitting which is much smaller than the bare tunneling amplitude Δ_0. Third, and most significantly, the interaction gives rise to collective motion of the defect ions, resulting in a zero-frequency peak in the motional spectrum (21); accordingly the dynamical susceptibility exhibits a relaxation peak.

The most convincing picture for relaxational motion involves reorientation of a large number of interacting dipoles. Therefore it is dominant at sufficiently high concentrations, where the average interaction energy exceeds the tunneling energy Δ_0, i.e., where $\mu > 1$ holds.

In the samples with lowest concentrations, 4 ppm of ^{7}Li and 6 ppm of ^{6}Li, the defects are well described as isolated two-level tunneling systems. With rising concentration, interactions become more important. As the most striking signature, we note the appearance of a relaxation peak (cf. Figs. 6 and 7).

B. Finite-energy excitations

According to the emergence of a zero-frequency feature, the relative spectral weight of the finite-energy excitations decreases when augmenting the defect density; at the same time the average excitation energy increases.

The shift to higher energies of the one-particle excitations may be explained by the molecular field of the surrounding defects. The interaction energy I_i, Eq. (22), acts as a dynamical asymmetry, leading to the characteristic dependence of the excitation energy $E_i=\sqrt{\Delta_0^2+I_i^2}$ and the corresponding residue in the correlation spectrum Δ_0^2/E_i^2. For the average excitation energy we find

$$\Delta_0\sqrt{1+\mu^2}=\sqrt{\Delta_0^2+\left(\frac{2}{3}\frac{np^2}{\varepsilon\varepsilon_0}\right)^2}. \tag{43}$$

The change of the excitation spectrum with defect density, as shown in Fig. 1 of Ref. 20, agrees well with both the temperature dependences of the resonant susceptibility shown in Figs. 6 and 7, and with specific heat measurements by Dobbs and Anderson.[11]

1. Resonant susceptibility

For isolated defects one expects the resonant susceptibility, Eq. (27), to increase linearly with concentration. Taking the dipolar interaction into account results in smaller residues of the one-particle excitations, and thus in a strong reduction of the resonant contribution to the susceptibility, as given by Eq. (31). (Hence the decrease of $\chi/\chi_{\rm iso}$ is a consequence of the reduced spectral weight of excitations with energy above 1 K.) In fact, such a behavior is found experimentally: Figures 6 and 7 show the resonant susceptibility to vary much weaker than linearly with defect density, and at the highest concentration investigated, it even decreases (cf. Fig. 7).

In Fig. 8 we compare the theoretical result (31) with experimental data as a function of the dimensionless coupling parameter μ, and thus of the defect density n, according to (20). At low concentration or $\mu\ll 1$, the susceptibility is that of isolated defects. With rising concentration interactions becoming more important, and as soon as the average dipolar energy $np^2/4\pi\varepsilon\varepsilon_0$ is comparable to the bare tunneling splitting Δ_0 (corresponding to $\mu\approx 1$), we observe a strong decrease in the resonant susceptibility. Figure 8 shows an almost perfect agreement of the experimental data with the theory given in Sec. II; this is valid for both isotopes ^{7}Li and ^{6}Li. (Because of the larger tunneling amplitude of the latter, a somewhat higher defect density is required in order to fulfill $\mu=1$.)

We would like to emphasize that the dipole moment p and the tunneling amplitude Δ_0 are the only parameters of our theory and that the values used for the fits have been taken from the literature.

At finite temperature, resonant and relaxational contributions may be separated through their different temperature dependences. The resonant susceptibility as a function of T reflects the thermal occupation of the energy levels. Figures 3, 4, 6, and 7 exhibit a variation according to $\tanh(E/2k_BT)$ as expected from the two-level tunneling model. At low concentrations the characteristic energy E is given by the tunneling amplitude Δ_0; at higher concentration it is shifted to the larger value $\Delta_0\sqrt{1+\mu^2}$.

2. Comparison with specific heat data

When measuring the specific heat arising from ^{6}Li and ^{7}Li defects at various concentrations ranging from 60 to 200 ppm, Dobbs and Anderson observed a broadening of the Schottky peak and a shift to higher temperature with rising defect density.[11] A fit with the pair model performed by these authors required too large values for the bare tunneling splitting. They deduced $^6\Delta_0/k_B=1.8$ K and $^7\Delta_0/k_B=1.25$ K instead of 1.65 K and 1.1 K as reported earlier.

According to (18), the pair model yields energies $\eta_\pm$ fulfilling $\eta_-<\Delta_0<\eta_+$. The broadening of the Schottky peak is easily explained by the distribution of the coupling parameter J. However, its shift is weak since the effects of the smaller energies η_- and the larger ones η_+ cancel in linear order in J. Only the second order yields a finite shift to higher temperature.

On the other hand, Mori theory yields a net increase of the average excitation energy even at low concentrations, besides the broadening of the energy distribution. Thus both effects are well accounted for by the density of states derived from Mori theory.

C. The relaxation peak

The reduction of the static susceptibility with rising concentration (cf. Fig. 8) is mainly due to the decreasing spectral weight of finite-energy excitations. The sum rule $\int d\omega G''(\omega)=\pi$ requires the appearance of an additional feature in the spectrum. In fact one finds, both theoretically and experimentally, a relaxation peak whose intensity increases with concentration, according to the decrease of the weight of the excitations in the range $\Delta_0\sqrt{1+\mu^2}$.

As discussed above, the factors K and r_0, Eq. (40), account quite well for the intensity of the relaxation peak in Figs. 6, 7, 9, and 10. For $\mu<1$ its relative weight increases according to (40); yet even at the highest concentrations, corresponding to $\mu\approx 1$, the resonant contribution in Figs. 6 and 7 exceeds by far the relaxational one. This may be explained by the small value for the parameter K, arising from the broad distribution of the rates.

Besides the height of the relaxation peak, the frequency dependence of the susceptibility (Fig. 12) hints on such a broad distribution of relaxation rates. This is displayed most clearly by the variation with time of the dielectric function after a sudden temperature change. At the lowest temperature investigated, the system needs more than an hour in order to reach equilibrium (Fig. 11). Such a relaxation spectrum covering many orders of magnitudes, and including very slow motions, has been derived theoretically from the dipolar interaction (cf. Fig. 4 of Ref. 20).

The relaxational susceptibility exhibit a maximum at about 100 mK. For reasonable parameters the logarithm in the denominator of (39) takes a value between $\frac{1}{30}$ and $\frac{1}{10}$, leading to the observed temperature T^* at which the maximum occurs.

According to (33), (38) relaxation should sharply disappear when decreasing the temperature well below T^*. Experimentally one rather finds a smooth maximum and signifi-

cant relaxational absorption even at the lowest temperatures investigated, $T=10$ mK. This discrepancy may be traced back to our neglecting of the low-energy excitations when deriving (33) and (38). The single activation energy E retained there leads to a sharp decrease of all relaxation rates and thus of the relaxation susceptibility.

D. Low-energy excitations

The calculated density of states exhibits additional excitations at low energies, besides the main peak above 1 K, comprising a few percent of the correlation spectrum $G''(\omega)$. The existence of such states has been shown experimentally by means of rotary echoes arising from a strong external field with appropriate frequency.[26] Here we merely note that the low-temperature absorption indicates the presence of excitations with energy well below 1 K.

E. Isotope effect

The KCl:Li systems permit a thorough study of the dependence on the defect mass by comparing samples doped with similar concentrations of ^{6}Li and ^{7}Li, respectively. In the two-level description (14), only the bare tunneling splitting Δ_0 varies with the defect mass m. In the semiclassical WKB approximation, one finds $\ln(\Delta_0)\propto-\sqrt{m}$, which accounts qualitatively for the observed values $\Delta_0=1.1$ K for ^{7}Li and $\Delta_0=1.65$ K for ^{6}Li.

Here we discuss the isotope effect of (a) the susceptibility of isolated defects at low concentration, (b) the crossover to relaxation dynamics, and (c) the maximum temperature of the relaxation peak.

(a) According to (27), the static susceptibility of isolated defects scales with $1/\Delta_0$ at low temperature $k_BT\ll\Delta_0$, and is independent of Δ_0 in the opposite limit $\Delta_0\ll k_BT$. This behavior is displayed in Fig. 3. Despite the slightly higher concentration of ^{6}Li, the low-temperature susceptibility of the ^{6}Li sample is smaller due to the factor $1/\Delta_0$ in (27), whereas at high temperature the susceptibility is proportional to the defect concentration.

(b) The crossover to relaxation dynamics is governed by the ratio μ of average coupling energy and bare tunneling splitting, which scales with $1/\Delta_0$. Figure 8 confirms the isotope effect expected from (20).

(c) At not too high defect concentration, the maximum temperature of the relaxation peak T^*, Eq. (39), varies linearly with the tunneling splitting Δ_0. Figure 5 provides strong evidence for the validity of this law.

VI. SUMMARY

Investigating crystals with defect concentrations between 4 ppm and 1100 ppm, we have shown the existence of a crossover in the dynamical behavior from coherent tunneling of isolated defects to collective relaxational motion, as predicted by Mori theory. The essential parameter is given by the ratio of the average dipolar interaction energy and the bare tunneling splitting. Here we briefly summarize the main results.

(a) At very low concentration we observe exactly the behavior expected for isolated defects in two-level approximation. However, the susceptibility per defect is reduced drastically, when rising the defect concentration above 100 ppm. Figure 8 shows a remarkably good agreement between theory and experiment.

(b) The relaxation peak indicates collective motion. Both the maximum temperature and the height are at least qualitatively accounted for by theory.

(c) Comparing the data for ^{6}Li and ^{7}Li reveals a characteristic isotope effect, which for most quantities agrees with that derived theoretically.

(d) For high concentration, both time- and frequency-dependent measurements indicate a broad spectrum of relaxation times, including values of about 1 h at the lowest temperatures investigated, in accordance with the relaxation spectrum derived in a mode-coupling approximation.

There remain two open questions: First, a more thorough investigation of the relaxation spectrum, both theoretically and experimentally, would permit a detailed understanding of the collective defect motion. This seems particularly interesting since at low temperature, the simple KCl:Li system shows features which are typical for glassy dynamics. Second, up to now little is known about the density of states in the energy range far below 1 K, which is governed by excitations of nearby pairs of lithium defects. These pairs constitute a unique system showing tunneling of strongly coupled atoms.

ACKNOWLEDGMENTS

The authors would like to thank the Crystal Growth Laboratory of the University of Utah for growing the samples and A.C. Anderson for providing two crystals previously investigated at the University of Illinois. We are grateful to F. Lüty, R.O. Pohl, M.v. Schickfus, and G. Weiss for many useful discussions. Part of this work has been financially supported by the Deutsche Forschungsgemeinschaft (Contract No. En299/1-1).

*Present address: Max-Planck-Institut für Festkörperforschung, Heisenbergstr. 1, 70569 Stuttgart, Germany.
†Present address: Institut Laue-Langevin, B. P. 156X, 38042 Grenoble, France.

[1] V. Narayanamurti and R.O. Pohl, Rev. Mod. Phys. **42**, 201 (1970).
[2] F. Bridges, Crit. Rev. Solid State Sci. **5**, 1 (1975).
[3] N.E. Byer and H.S. Sack, J. Phys. Chem. Solids **29**, 677 (1968).
[4] M. Gomez, S.P. Bowen, and J.A. Krumhansl, Phys. Rev. **153**, 1009 (1967).
[5] F. Holuj and F. Bridges, Phys. Rev. B **27**, 5286 (1983); X. Wang and F. Bridges, *ibid*. **46**, 5122 (1992).
[6] J.P. Harrison, P.P. Peressini, and R.O. Pohl, Phys. Rev. **171**, 1037 (1968).
[7] A.T. Fiory, Phys. Rev. B **4**, 614 (1971).
[8] K. Knop and W. Känzig, Phys. Kondens. Mater. **15**, 205 (1972); Helv. Phys. Acta **46**, 889 (1974).
[9] R.C. Potter and A.C. Anderson, Phys. Rev. B **24**, 677 (1981).
[10] D. Moy, R.C. Potter, and A.C. Anderson, J. Low Temp. Phys. **52**, 115 (1983).
[11] J.N. Dobbs and A.C. Anderson, Phys. Rev. B **33**, 4172 (1986).
[12] M.W. Klein, Phys. Rev. **141**, 489 (1966).
[13] W.N. Lawless, Phys. Kondens. Mater. **5**, 100 (1966).
[14] M.E. Baur and W.R. Salzman, Phys. Rev. **178**, 1440 (1969).

[15] M.W. Klein, Phys. Rev. B **29**, 5825 (1984); **31**, 2528 (1985).
[16] M.W. Klein, Phys. Rev. B **40**, 1918 (1989).
[17] T. Kranjc, J. Phys. A **25**, 3065 (1992).
[18] O. Terzidis and A. Würger, Z. Phys. B **94**, 341 (1994).
[19] A. Würger, Z. Phys. B **94**, 173 (1994).
[20] A. Würger, Z. Phys. B **97**, 561 (1995).
[21] M. Tornow, R. Weis, G. Weiss, C. Enss, and S. Hunklinger, Physica B **194-196**, 1063 (1994).
[22] Note that the Li concentrations of the samples labeled by mistake as 2% and 0.5% were actually much lower as determined using flame emission spectroscopy. Data from these two samples are not included in the present work.
[23] R.J. Quigley and T.P. Das, Phys. Rev. **164**, 1185 (1967).
[24] C. Enss, H. Schwoerer, D. Arndt, M.v. Schickfus, and G. Weiss, Europhys. Lett. **26**, 289 (1994).
[25] C. Enss, H. Schwoerer, D. Arndt, and M.v. Schickfus, Phys. Rev. B **51**, 811 (1995).
[26] R. Weis, C. Enss, B. Leinböck, G. Weiss, and S. Hunklinger, Phys. Rev. Lett. **52**, 2220 (1995).
[27] In order to link with the notation used in Refs. 19 and 20, note the identity $\frac{2}{3}np^2/\varepsilon\varepsilon_0 \equiv cJ_2 \equiv I_c$.
[28] For the sake of simplicity, we have discarded the irrelevant poles $\varepsilon_+^{(i)}$ and changed the notation used in Ref. 20 according to $\varepsilon_-^{(i)} \rightarrow E_i$, $R_-^{(i)} \rightarrow (1-R_i)$, $R_0^{(i)} \rightarrow R_i$, $\gamma_-^{(i)} \rightarrow \Gamma_i$, and $\gamma_0^{(i)} \rightarrow \gamma_i$.
[29] As an example the level of OH^- and other impurities in the 4 ppm sample has been carefully checked using low-temperature Fourier spectroscopy by Professor F. Lüty at the University of Utah. The concentration of OH^- in this crystal turned out to be only 0.14 ppm. The level of all other impurities like CN^- detectable with this technique was even below that concentration.
[30] H. Fröhlich, *Theory of Dielectrics* (Oxford University Press, New York, 1957).
[31] M.C. Robinson and A.C. Hollis Hallett, Can. J. Phys. **44**, 2211 (1966).
[32] R.A. Brand, S.A. Letzring, H.S. Sack, and W.W. Webb, Rev. Sci. Instrum. **42**, 927 (1971).
[33] To calculate the susceptibility of the 4 ppm and 60 ppm ^{7}Li sample we accounted for the 7.4% ^{6}Li of the natural isotope mixture. This leads only to a small variation, but to a still noticeable better agreement of fit and data.
[34] J.A. Süssmann, Phys. Condens. Matter **2**, 146 (1964); J. Phys. Chem. Solids **28**, 1643 (1967).